

Sodium-Dependent Movement of Covalently Bound FMN Residue(s) in Na⁺-Translocating NADH:Quinone Oxidoreductase

Michael I. Verkhovsky,^{||,⊥} Alexander V. Bogachev,^{*,†} Andrey V. Pivtsov,[‡] Yulia V. Bertsova,[†] Matvey V. Fedin,[§] Dmitry A. Bloch,^{||} and Leonid V. Kulik^{*,‡}

[†]Department of Molecular Energetics of Microorganisms, A.N. Belozersky Institute of Physico-Chemical Biology, Moscow State University, Moscow 119992, Russia

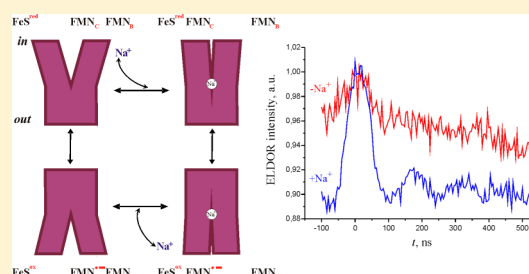
[‡]Institute of Chemical Kinetics and Combustion, Russian Academy of Sciences, 630090, Novosibirsk, Russia

[§]International Tomography Center, Russian Academy of Sciences, 630090, Novosibirsk, Russia

^{||}Helsinki Bioenergetics Group, Institute of Biotechnology, P.O. Box 65, (Viikinkaari 1), 00014 University of Helsinki, Helsinki, Finland

Supporting Information

ABSTRACT: Na⁺-translocating NADH:quinone oxidoreductase (Na⁺-NQR) is a component of respiratory electron-transport chain of various bacteria generating redox-driven transmembrane electrochemical Na⁺ potential. We found that the change in Na⁺ concentration in the reaction medium has no effect on the thermodynamic properties of prosthetic groups of Na⁺-NQR from *Vibrio harveyi*, as was revealed by the anaerobic equilibrium redox titration of the enzyme's EPR spectra. On the other hand, the change in Na⁺ concentration strongly alters the EPR spectral properties of the radical pair formed by the two anionic semiquinones of FMN residues bound to the NqrB and NqrC subunits (FMN_{NqrB} and FMN_{NqrC}). Using data obtained by pulse X- and Q-band EPR as well as by pulse ENDOR and ELDOR spectroscopy, the interspin distance between FMN_{NqrB} and FMN_{NqrC} was found to be 15.3 Å in the absence and 20.4 Å in the presence of Na⁺, respectively. Thus, the distance between the covalently bound FMN residues can vary by about 5 Å upon changes in Na⁺ concentration. Using these results, we propose a scheme of the sodium potential generation by Na⁺-NQR based on the redox- and sodium-dependent conformational changes in the enzyme.



The Na⁺-translocating NADH:quinone oxidoreductase (Na⁺-NQR) is a redox-driven sodium pump that generates transmembrane electrochemical Na⁺ potential.¹ This enzyme has been shown to operate in the respiratory chain of various bacteria, including several pathogenic microorganisms.^{2,3} Despite a number of extensive biochemical and biophysical studies, the mechanism of the sodium potential generation by this enzyme is not known; this is in part hampered by the lack of 3D structure available for this enzyme. Na⁺-NQR consists of six subunits (NqrA-F)⁴ encoded by the six genes of the *nqr* operon.^{5,6} An FAD and a [2Fe–2S] cluster are bound to subunit NqrF; the latter also possesses a binding motif for NADH.^{5,7,8} Besides, two FMN residues are covalently bound via the phosphoester bonds to threonine residues in subunits NqrB and NqrC (FMN_{NqrB} and FMN_{NqrC}, respectively).^{2,9,10} The enzyme was also reported to possess a noncovalently bound riboflavin,^{11,12} and its binding site on the NqrB subunit has been recently discovered.¹³

Under equilibrium conditions, the flavin cofactors of Na⁺-NQR reveal three distinct, EPR-detectable radical signals: (i) the oxidized enzyme contains a neutral radical most likely due to riboflavin;^{12,14–17} (ii) the fully reduced Na⁺-NQR reveals an anionic flavin radical arising from FMN_{NqrB},^{12,14–17} (iii) under

weakly reducing conditions ($E_h \cong -260$ mV vs SHE), the enzyme reveals another anionic radical, which was assigned to the FMN_{NqrC} semiquinone.^{17,18}

As shown by the stopped-flow optical spectroscopy, the kinetics of Na⁺-NQR reduction by NADH displays several distinct phases corresponding to the reduction of different flavin species.¹ The sequence of the phases can be subdivided into two parts regarding their position in the catalytic cycle relative to a step where coupling between a particular redox reaction and the Na⁺ translocation may occur (a “coupling step”). The first part (*before the coupling step*) consists of the fast, Na⁺-independent hydride ion transfer from NADH to FAD (phase I) followed by the partial electron separation and the formation of the equivalent fractions of the reduced [2Fe–2S] cluster and FAD neutral semiquinone radical (phase II).¹⁹ The second part (*after the coupling step*) consists of the three phases, which kinetics are strongly dependent on [Na⁺] and which may reflect the reduction of different flavin cofactors.^{14,15,20} The fastest Na⁺-dependent phase (phase III)

Received: March 7, 2012

Revised: May 24, 2012

Published: June 15, 2012



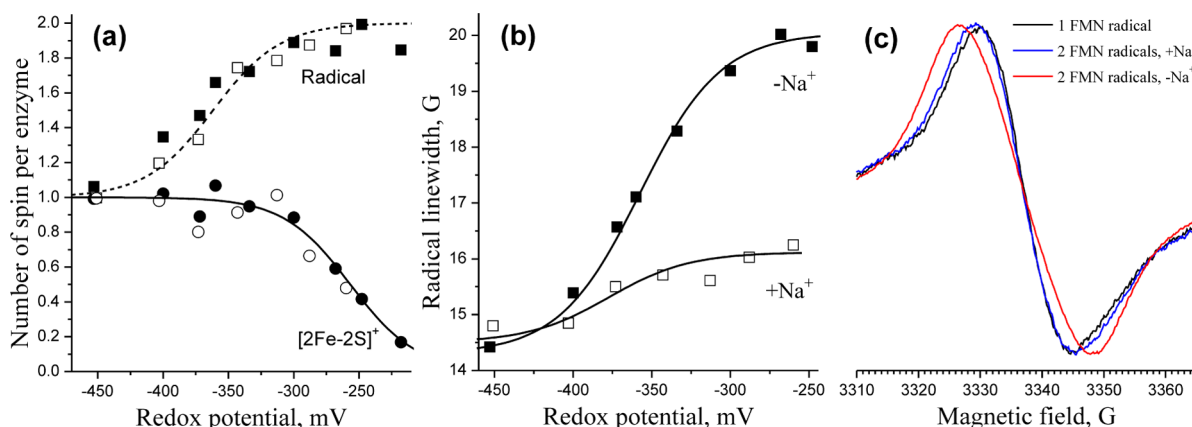


Figure 1. X-band EPR spectroelectrochemical redox titration of Na⁺-NQR at pH 9.5. (a) Spin concentration in signals from the flavin radicals (squares) and [2Fe-2S] cluster (circles). 100 mM Na⁺ (open symbols) or no Na⁺ (closed symbols) is present. Lines are the results of the best one-electron, Nernstian curve fits with $E_m = -360$ mV (dashed line) and $E_m = -260$ mV (solid line). The total number of radicals per enzyme molecule was quantified as in ref 18. (b) Peak-to-peak spectral line width of the radical signal. 100 mM Na⁺ (open symbols) or no Na⁺ (closed symbols) is present. Lines are the results of the best one-electron, Nernstian curve fits with $E_m = -360$ mV. (c) Normalized spectra of the radical signal at $E_h = -460$ mV (black line), $E_h = -260$ mV in the presence of Na⁺ (blue line), and $E_h = -260$ mV in the absence of Na⁺ (red line). The spectra were normalized on the equal amplitude. Conditions: microwave frequency, 9.369 GHz; temperature, 80 K; microwave power, 10 μ W; modulation amplitude, 4 G. All redox potentials quoted refer to SHE.

corresponds to one-electron reduction of riboflavin neutral semiquinone.^{15,20} The following phase IV consists of one-electron reduction of FMN_{NqrB} and FMN_{NqrC} yielding two anionic semiquinones.^{15,20} The last phase V is the one-electron reduction of the earlier formed FMN_{NqrC} radical to the fully reduced flavin.²⁰ It has been proposed that the electron transport from the [2Fe-2S] cluster to FMN_{NqrC} is the redox step which is coupled to the binding of Na⁺ prior to its further pumping.^{1,20}

To determine the coupling mechanism of Na⁺-NQR, it is very important to reveal the origin of the strong sodium concentration dependence of the electron transport from the [2Fe-2S] cluster to FMN_{NqrC}. It was proposed earlier that such effect can be caused by the sodium dependence of thermodynamic properties of at least one prosthetic group of the enzyme.²¹ However, all determined equilibrium redox transitions in Na⁺-NQR have been found essentially [Na⁺]-independent.^{18,22,23} There is another plausible explanation for the sodium dependence of the electron transport in Na⁺-NQR: rather than *redox potential* of a prosthetic group is [Na⁺]-dependent, the *distance* (and, hence, the electron transport rate) between prosthetic groups is altered by Na⁺ binding to the enzyme. To test the latter hypothesis, in the present study we determined the interspin distance between the two covalently bound FMN residues using pulse EPR measurements in the absence and in the presence of sodium ions. We showed that this distance alters for about 5 Å upon changes in Na⁺ concentration.

MATERIALS AND METHODS

Enzyme Purification. His-tagged Na⁺-NQR from *Vibrio harveyi* was purified using affinity chromatography as earlier described.¹⁸

Sodium concentration was measured by flame photometry.

Equilibrium Redox Titration of X-Band EPR Spectra. X-band EPR spectroelectrochemical redox titration was accomplished as described previously.¹⁸ The sample contained 40 μ M Na⁺-NQR, 100 mM KCl or NaCl, 12% (v/v) glycerol, 0.1% DDM, 100 mM BTP-HEPES (pH 9.5), and redox mediators

(200 μ M cobalt(III) sepulchrate, $E_m = -350$ mV, 400 μ M pentaamminechlororuthenium, $E_m = -130$ mV, and 200 μ M hexaammineruthenium, $E_m = +50$ mV). The sample (ca. 0.3–0.4 mL) was placed into an all-glass electrochemical apparatus,^{18,24} degassed using a locally built vacuum line, and filled with He gas; then the traces of oxygen were further quenched electrochemically by poisoning the potential at -400 mV. Then a succession of different E_h values was applied to obtain a redox titration curve. At each E_h the onset of equilibrium was checked, as the changes in the cell current became no longer significant, and the apparatus was tipped to transfer the sample to the EPR tube; the sample was then transferred back to the electrochemical compartment, and the stability in the ambient potential was checked. Then the sample was finally transferred to the EPR tube and immediately frozen in liquid nitrogen for the EPR spectroscopy. The procedure was repeated at each E_h value. A PAR263A potentiostat (Princeton Applied Research) was employed to poise the desired potential. All redox potentials quoted refer to the SHE.

Samples for Pulse EPR Spectroscopy. Two Na⁺-NQR samples were used for pulse EPR experiments. Both samples were poised at redox potential of -260 mV (pH 9.5) in the spectroelectrochemical apparatus as described above, except that 300 μ M Na⁺-NQR was used. One sample was prepared in the presence of 100 mM NaCl ("sodium sample"), while the other in the presence of 100 mM KCl ("sodium-free sample", residual sodium concentration was about 40 μ M as was checked by the flame photometry).

X-band CW EPR spectroscopy was accomplished using a Bruker ESP-300 spectrometer. The field modulation frequency was 100 kHz. The temperature of the sample (80 K) was controlled by an ESR 900 cryostat with an ITC4 temperature controller (Oxford Instruments).

X-Band Pulse EPR Spectroscopy. Pulsed EPR and ELDOR experiments were performed using an Elexsys-580 FT EPR spectrometer equipped with a dielectric cavity (Bruker ER 4118 X-MD-5) inside an Oxford Instruments CF 935 cryostat, which was cooled by nitrogen flow. The echo-detected (ED) EPR spectra were recorded using two-pulse sequence $\pi/$

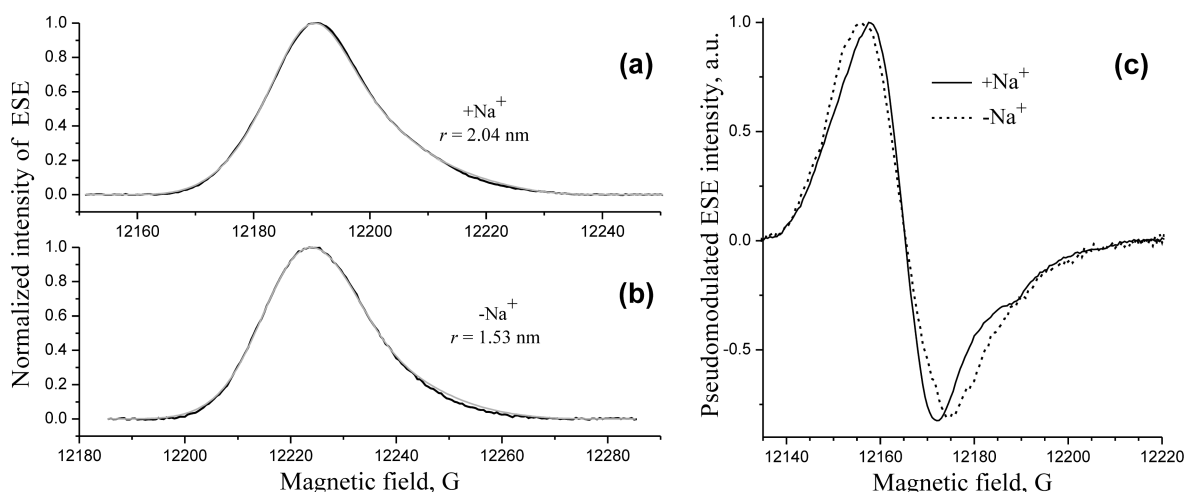


Figure 2. Q-band two-pulse echo-detected EPR spectra of Na^+ -NQR. (a, b) Spectra in the presence (a) and in the absence (b) of Na^+ , respectively. Experimental (black lines) and simulated (gray lines) spectra are shown. (c) Q-band CW-like EPR spectra were obtained by numerical pseudomodulation of the experimental spectra shown on (a) (sodium sample, solid line) and (b) (sodium-free sample, dashed line), respectively. For pseudomodulation the 4 G amplitude was used. The spectrum without Na^+ is shifted by 22.5 G to match the center of the spectrum in the presence of Na^+ . Conditions: duration of π -pulse, 800 ns; interpulse delay $\tau = 1500$ ns; temperature, 80 K. The dipolar frequency ν_d is 6 MHz for the sample with Na^+ (corresponds to the interspin distance between the flavin radicals, $r = 20.4$ Å) and 14 MHz for the sample without Na^+ (corresponds to the interspin distance between the flavin radicals $r = 15.3$ Å). The difference in resonance magnetic fields in panels a and b is caused by the difference in working microwave frequency. 100 mM Na^+ is present, where indicated. For other conditions, see Materials and Methods.

$2-\tau-\pi-\tau$ -echo with the duration of a π -pulse, 48 ns, and the interpulse delay, 120 ns. For the pulse ELDOR experiments the four-pulse sequence²⁵ (detection $\pi/2-\tau-\pi-(\tau+\tau_1)-\pi-\tau_1$ -echo, pump π -pulse scanned during $\tau+\tau_1$ interval) was used with $\tau = 200$ ns, $\tau_1 = 600$ ns, and the duration of $\pi/2$ and π microwave pulses of 24 and 48 ns, respectively. The difference between the detection and pump microwave frequencies was 70 MHz.

For pulse proton ENDOR experiments a dielectric ENDOR resonator (Bruker EN 4118X-MD4) was used. The Davies ENDOR microwave pulse sequence $\pi-T-\pi/2-\tau-\pi-\tau$ -echo was used, with a radio-frequency (rf) π pulse applied during the T -interval. The durations of $\pi/2$ and π microwave pulses were 100 and 200 ns, respectively. The τ value was 300 ns, and the T value was 20 μ s. The rf pulse was amplified by a 150 W rf amplifier. The π rf pulse of 14 μ s duration was placed 1 μ s after the first π microwave pulse of the pulse sequence.

Q-Band Pulse EPR Spectroscopy. Q-band ED EPR spectra were measured using an X/Q-band FT EPR spectrometer Bruker Elexsys E580 equipped with an ER 5106QT resonator inside an Oxford Instruments CF 935 cryostat. The coupling of the resonator with the waveguide was close to the critical one with Q -value of about 1500. Two-pulse sequence $\pi/2-\tau-\pi-\tau$ -echo with duration of microwave π -pulse 800 ns and interpulse delay 1500 ns was used. The long microwave pulses were used to increase the resolution of ED EPR spectra.

In all pulse EPR experiments the shot repetition time was chosen to allow the echo signal to restore between the consecutive pulse trains. The echo signal in the time domain was integrated. In all experiments the temperature was 80 K.

RESULTS

In this work, the equilibrium redox titration of the EPR spectra of Na^+ -NQR from *Vibrio harveyi* was performed within the range between -460 and -220 mV vs SHE at pH 9.5 in the absence and in the presence of Na^+ (Figure 1). The alkaline

conditions were chosen to increase the stability constant for the FMN_{NqrC} semiquinone and to avoid overlapping between the redox transitions of the $[\text{2Fe-2S}]$ cluster and FMN_{NqrC} .^{23,26} The fully reduced enzyme ($E_h \leq -450$ mV) is known to contain two prosthetic groups in the paramagnetic state: these are the reduced $[\text{2Fe-2S}]$ cluster and the anionic radical of FMN_{NqrB} .^{12,14-17} As shown in Figure 1a, gradual oxidation of the fully reduced Na^+ -NQR caused about 2-fold increase in the spin concentration in radical signal at $E_h > -300$ mV due to the formation of the semiquinone form of FMN_{NqrC} .^{17,18,23} In accordance with previously made predictions,²³ FMN_{NqrC} revealed one-electron oxidation with $E_m \approx -360$ mV at pH 9.5, and this process did not depend on Na^+ concentration (Figure 1a). The subsequent rise of redox potential resulted in one-electron oxidation of the $[\text{2Fe-2S}]$ cluster with $E_m \approx -260$ mV, again without any effect of Na^+ (Figure 1a).

As was shown previously,^{18,26} the FMN_{NqrB} and FMN_{NqrC} residues are located in Na^+ -NQR close to each other. Thus, the paramagnetic state of both centers results in broadening of their EPR spectra due to dipole-dipole interaction.^{18,26} The redox potential dependence of the peak-to-peak line width of the Na^+ -NQR radical is shown on Figure 1b. In the presence of Na^+ the enzyme oxidation from -460 to -220 mV led to the slight increase in line width of the radical signal from 14.5 to 16 G. Surprisingly, in the absence of Na^+ this effect was much more pronounced: the radical line width increased from 14.5 to 20 G (the initial and final radical spectra are shown in Figure 1c). It is noteworthy that in both cases the E_h dependence of radical line width was well fitted by Nernstian curves for one-electron transition ($n = 1$) with $E_m = -360$ mV (see Figure 1b), i.e., by the same process that led to the increase in spin concentration of the radical signal (see Figure 1a). In other words, the radical signal broadening correlated with the formation of semiquinone form of FMN_{NqrC} .

These results indicate that the redox properties of the studied Na^+ -NQR prosthetic groups are not affected by the presence of sodium ions in the reaction medium (Figure 1a; see also refs

18, 22, and 23), but the EPR spectral properties of the FMN_{NqrC} and/or FMN_{NqrB} semiquinones are significantly altered (Figure 1b,c). The radical signal broadening in the absence of Na^+ , as compared with its high concentration, can be caused by one of the following reasons: (i) $[\text{Na}^+]$ -dependent change in the g -tensor of one or both flavin radicals; (ii) $[\text{Na}^+]$ -dependent change in electron spin density distribution within flavin anion radicals with corresponding change of hyperfine coupling with protons and nitrogen nuclei; (iii) $[\text{Na}^+]$ -dependent change in the distance between one or both flavin radicals and the $[2\text{Fe}-2\text{S}]$ cluster, respectively, with the corresponding change in the electron–electron dipole interaction of flavin radical(s) and the $[2\text{Fe}-2\text{S}]$ cluster; (iv) $[\text{Na}^+]$ -dependent change in the distance between flavin radicals with the corresponding change in the electron–electron dipole interaction between them.

To determine which is the reason for the broadening of the radical signal in Na^+ -NQR at low sodium concentrations, two samples of the enzyme were poised at $E_h = -260$ mV, pH 9.5, in the presence of 100 mM KCl or 100 mM NaCl (“sodium-free” and “sodium” samples, respectively). As can be deduced from Figure 1a, both samples contained ca. 2 flavin radicals and ~ 0.5 paramagnetic $[2\text{Fe}-2\text{S}]$ clusters per enzyme (CW X-band EPR spectra of the samples are shown in the Supporting Information, Figure S1). These samples were further analyzed using pulse EPR spectroscopy.

In principle, local electric fields induced by Na^+ charge could cause $[\text{Na}^+]$ -dependent change of g -tensor. A similar effect is known for nitroxide radicals with ionizable groups from high-field EPR study.²⁷ The change of principal g -tensor values on the order of 10^{-4} – 10^{-3} was detected upon protonation/deprotonation of nitroxide radicals,²⁷ and such effect could be expected for flavin radicals in Na^+ -NQR upon sodium binding. To test this possibility (possibility i), the Q-band echo-detected EPR spectra of flavin radicals were measured for the sodium and sodium-free samples (Figure 2). Both spectra are similar to the previously reported X-band ED EPR spectra of flavin radicals,^{18,26} although, in contrast to X-band, slight asymmetry of the spectra can be noticed in Q-band (Figure 2a,b). This is caused by the increased contribution of g -tensor anisotropy to the EPR spectrum shape at Q-band. As expected, the Q-band spectra of both samples were quite similar; however, the spectrum of the sodium-free sample appears to be broader than of the sodium sample. This difference is clearly seen in Figure 2c, which shows Q-band EPR spectra obtained by numerical pseudomodulation of the echo-detected EPR spectra presented in Figure 2a,b. The peak-to-peak line width increased from 14.5 G in the sodium sample to 19 G in the sodium-free sample. Thus, the difference of line width between the samples is 4.5 G, which is nearly the same as in X-band (see Figure 1b,c). These data argue against possibility i, as a strong influence on the EPR line width is expected for Q-band in the case of $[\text{Na}^+]$ -dependent change of g -tensor anisotropy.

To test possibility ii, the X-band pulse proton Davies-ENDOR spectra in both samples were measured. As shown in Figure 3, the spectra of the sodium-free and sodium samples were very similar and resemble previously reported proton ENDOR spectra of flavin anion radicals in Na^+ -NQR.^{17,26} This indicates that in both samples either FMN_{NqrB} or FMN_{NqrC} is in the anionic semiquinone form. Some differences in the intensity of the central peaks in the ENDOR spectra probably originate from slight difference of the amplitude of mW pulses for the sodium and sodium-free samples. The amplitude of mW pulses

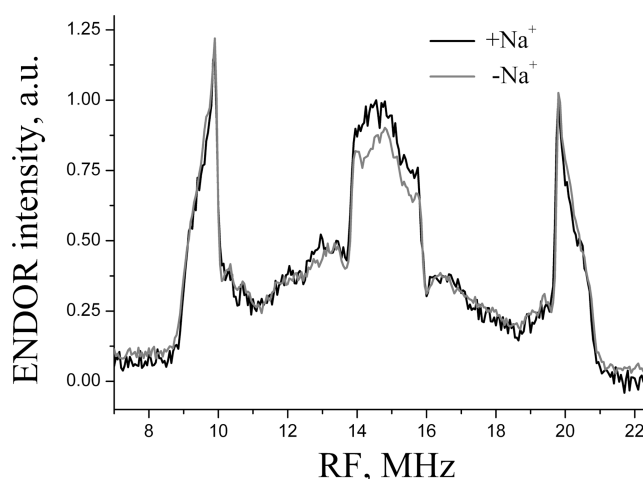


Figure 3. X-band Davies ENDOR spectra of flavin radicals in Na^+ -NQR. Black and gray lines are for sodium sample and sodium-free sample, respectively. B_0 corresponds to the maximum of echo-detected EPR spectrum for each sample. The duration of microwave $\pi/2$ pulse was 100 ns, duration of rf π pulse was 14 μs . Temperature, 80 K. 100 mM Na^+ is present, where indicated. The spectra were normalized to the intensity of the outermost peaks. For other conditions, see Materials and Methods.

is known to affect the intensity of Davies ENDOR signal for small HFI constants.²⁸ To compare the central regions of the ENDOR spectra around the proton Larmor frequency, the Mims ENDOR spectra for both samples were measured. As can be seen in Figure S2, the spectral features of Mims ENDOR spectra for the sodium-free and sodium samples have the same frequencies. All these data imply that the proton hyperfine interactions (HFI) tensors for the radicals are the same for both samples, and no substantial redistribution of spin density within isoalloxazine rings of covalently bound flavins occurs upon change in Na^+ concentration.

The significant alteration of nitrogen HFI constants is also unlikely, as was revealed by two-pulse ESEEM (see Figures S4 and S6). It is interesting to note that the ESEEM spectrum of the sodium sample compared to the sodium-free sample contains two additional peaks with frequencies 3.7 and 7.4 MHz (see Figure S6). These frequencies are close to Larmor and double Larmor frequencies of ^{23}Na nuclei at a typical magnetic field of our X-band experiments $B_0 = 3470$ G (3.9 and 7.8 MHz, respectively). Since modulation with such frequencies is expected for the case of ^{23}Na nuclei weakly interacting with flavin radicals,²⁹ this could point to the presence of Na^+ in the proximity of these radicals in Na^+ -NQR. Further experiments are required to test this possibility.

In summary, the data obtained by ENDOR and ESEEM indicate that the radical line width broadening in the absence of Na^+ cannot be explained by change in electron spin density distribution within flavin anion radicals.

Possibility iii is also unlikely because the proximity of the $[2\text{Fe}-2\text{S}]$ cluster to FMN semiquinone(s) would cause the change of electron spin relaxation properties of the radical(s). However, virtually no difference between the inversion-recovery traces was detected for the radical signal in the two samples studied at X-band (Figure 4; for details see Figures S3 and S4). Moreover, X-band microwave power saturation curves were nearly the same for the radical signal in the sodium and sodium-free samples (see Figure S5). It is also noteworthy that the redox profile of the radical spectrum broadening correlated

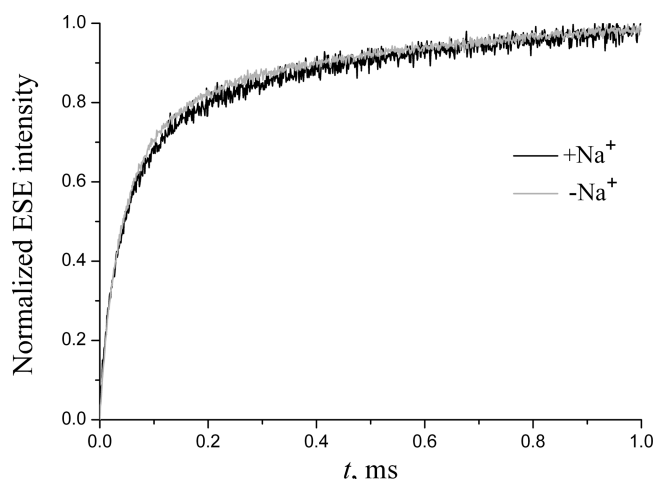


Figure 4. Inversion-recovery traces of flavin radicals in the sodium (black line) and sodium-free (gray line) Na^+ -NQR samples. The traces were taken at the constant magnetic field B_0 , corresponding to the maximum of EPR spectra, at 80 K. The microwave pulse sequence was $\pi-T-\pi/2-\tau-\pi-\tau-\text{echo}$, with $\tau = 120$ ns, duration of π -pulse was 32 ns. 100 mM Na^+ is present, where indicated.

only with FMN_{NqrC} titration, not with titration of the $[2\text{Fe}-2\text{S}]$ cluster (see Figure 1).

Thus, we can exclude the first three possibilities and propose that the change of the distance between the two FMN radicals in Na^+ -NQR is the most plausible reason for the EPR spectra difference of the sodium and sodium-free samples.

To determine the distance between the paramagnetic species in nanometer range, pulse ELDOR spectroscopy is often used.^{30–33} The black and gray lines in Figure 5 show X-band pulse ELDOR time traces for sodium and sodium-free samples,

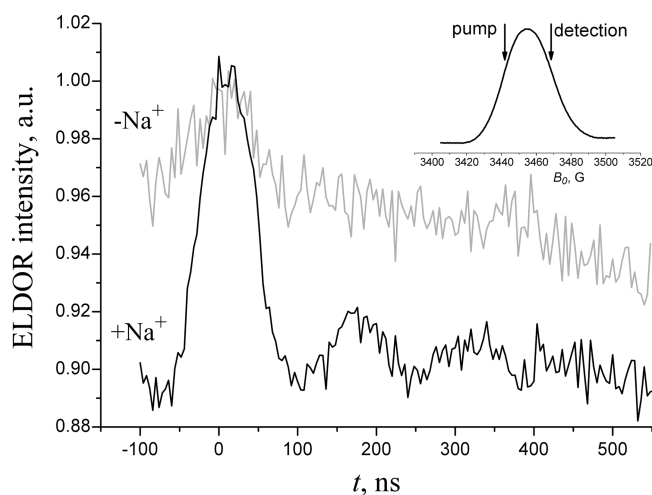


Figure 5. X-band four-pulse ELDOR traces of Na^+ -NQR for sodium sample (black line) and for sodium-free sample (gray line). Microwave frequency offset $\nu_{\text{detection}} - \nu_{\text{pump}} = 70$ MHz. Duration of π -pulse 48 ns. Shot repetition time, 1 ms. Temperature, 80 K. Inset: X-band two-pulse ED EPR spectrum of sodium-free sample, detected with interpulse interval $\tau = 120$ ns. The ED EPR spectrum of the sodium sample detected at the same conditions was very similar (data not shown). The arrows show magnetic field positions corresponding to microwave pump and detection in the pulse ELDOR experiment. 100 mM Na^+ is present, where indicated. For other conditions, see Materials and Methods.

respectively, obtained with the four-pulse sequence.²⁵ The traces were normalized to the unity intensity at $t = 0$ ns. This allows comparison of the magnitude of the ELDOR effect in the studied samples.³⁴ Relatively deep modulation with the main frequency of about 6 MHz was obtained in the ELDOR trace for the sodium sample. Assuming that the modulation frequency corresponds to the main dipolar frequency $\nu_d = \omega_d / 2\pi$, we can use the relation (eq 1) to determine the distance between the Na^+ -NQR radicals in the sodium sample:

$$\omega_d = \frac{g_1 g_2 \beta^2}{\hbar r^3} \quad (1)$$

where ω_d is dipolar frequency in angular frequency units, g_1 and g_2 are g -factors of the flavin radicals (both are close to the free electron g -value), β is the Bohr magneton, \hbar is the reduced Planck constant, and r is the distance between the spins in point-dipole approximation. From eq 1 we obtain $r = 20.4$ Å. Note that the same system has been recently studied by ELDOR,²⁶ and $\nu_d = 5$ MHz was determined. Taking into account better signal-to-noise ratio of the ELDOR trace in the present study, we conclude that the value $\nu_d = 6$ MHz is more precise. The cosine Fourier transform spectrum of the dipolar modulation for the sodium sample is shown at Figure 6. The

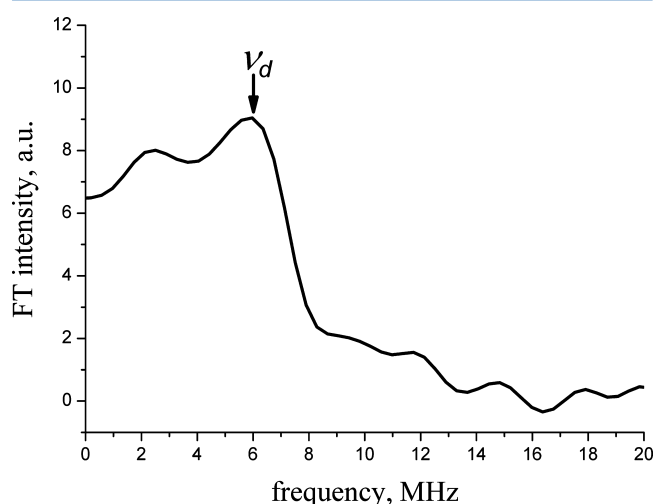


Figure 6. Cosine Fourier transform spectrum of the dipolar modulation caused by the interaction of the flavin radicals in the sodium sample of Na^+ -NQR (ELDOR trace from Figure 5).

spectrum has the characteristic shape of dipolar modulation pattern; the maximum at 6 ± 1 MHz corresponds to ν_d . The accuracy of the dipolar frequency is estimated from the width of the main peak in Figure 6, which corresponds to ν_d . Because of the limited interval of the dipolar evolution in our experiment, it is difficult to draw the conclusion about the possible distribution of the interspin distance. However, from the relatively slow dipolar modulation decay it is clear that for the majority of Na^+ -NQR in the sodium sample the r value is in the range 20.4 ± 1 Å.

In contrast, no modulation was detected for the ELDOR trace from the sodium-free sample. Moreover, the initial drop in the intensity for $t < 100$ ns was about 3 times smaller for the sodium-free sample than for the sodium sample. The absence of the dipolar modulation and the overall decrease of the ELDOR amplitude for the sodium-free sample suggest that the interspin distance between the radicals is too small in this probe and that

the dipolar frequency ω_d in this case does not fulfill the condition necessary for observation of dipolar modulation in pulse ELDOR experiment:

$$\omega_d < \gamma B_1$$

where γ is free electron gyromagnetic ratio and B_1 is oscillating magnetic field of the mW pulse.³⁵ The amplitude of the magnetic field in our pulses (in frequency units) $\omega_1 = \gamma B_1 \approx 2\pi \times 10$ MHz was estimated from the 48 ns duration of the π -pulse.

The difference between ELDOR time traces for the sodium and sodium-free samples points directly on the change in the distance between the flavin radicals in Na⁺-NQR at different Na⁺ concentrations. However, for the sodium-free sample it was not possible to determine this distance from the pulse ELDOR experiment. Therefore, this value was obtained from the numerical simulation of Q-band ED EPR spectra of flavin radicals for the sodium and sodium-free samples. We preferred to simulate Q-band ED EPR spectra instead of X-band CW EPR spectra because the former are free from the contribution of the paramagnetic [2Fe–2S] cluster, which completely decays in our experiments due to its short T_2 .

For the simulation, the spin Hamiltonian of a pair of interacting electron spins of flavin radicals was used:

$$\begin{aligned} \hat{H} = & \beta S_{g1} B_0 + \beta S_{g2} B_0 + S_1 A_{N(5)}^1 I_{N(5)}^1 + S_1 A_{N(10)}^1 I_{N(10)}^1 \\ & + S_2 A_{N(5)}^2 I_{N(5)}^2 + S_2 A_{N(10)}^2 I_{N(10)}^2 + S_1 D S_2 \end{aligned}$$

where g_1 , g_2 and S_1 , S_2 are g -tensors and electron spins of both radicals, respectively; $A_{N(5)}$ and $A_{N(10)}$ are nitrogen HFI tensors for N(5) and N(10), respectively (for atoms numbering in flavins, see Figure S7); $I_{N(5)}$ and $I_{N(10)}$ are nuclear spin operators for nitrogen atoms (¹⁴N, $I = 1$) in positions 5 and 10, respectively (upper indices denote the HFI with corresponding flavin radicals); D = tensor of dipole–dipole interaction with the principal values (ν_d , ν_d , $-2\nu_d$).

At the first step, the spectrum of the flavin radicals in the sodium sample was simulated under following assumptions. The equal g -tensors taken from ref 36 were used for both radicals. The HFI tensors for the nitrogen atoms N(5) and N(10) were also assumed to be equal for both radicals; their principal values were slightly varied compared to those in ref 36. The strength of the dipolar interaction between the electron spins of the radicals $\nu_d = 6$ MHz was fixed. All other magnetic interactions including HFI with protons of flavin radicals and matrix as well as electron–electron dipolar interaction of the flavin radicals with the spin of the [2Fe–2S] cluster were taken into account as the Gaussian broadening of the individual EPR lines, which width was varied. For simplicity all tensors were assumed collinear.

The numerical simulation was performed using EasySpin 3.1.1 package³⁷ run under the MATLAB interface. The powder-averaged EPR spectrum was calculated. For each orientation of the spin system the frequencies and intensities of EPR transitions were calculated exactly using the approach of full diagonalization of spin Hamiltonian. The best-fitted values are presented in Table S1. The variation of the orientation of the principal axes of dipolar, HFI, and g -tensor did not lead to the substantial change of the simulated spectrum. The result of the simulation of the Q-band ED EPR spectrum for the sodium sample (assuming that the interspin distance between radicals at these conditions is equal to 20.4 Å) is shown by the gray line

in Figure 2a; it can be seen that the simulation fits the experimental data well.

At the second step the Q-band EPR spectrum of the sodium-free sample was simulated using the same spin Hamiltonian and the set of magnetic parameters, except ν_d , which was varied for this case. The result of this simulation of Q-band ED EPR spectrum for the sodium-free sample is shown by the gray line in Figure 2b. The best fitted value was $\nu_d = 14$ MHz, which corresponds to point-dipolar interspin distance $r = 15.3$ Å. The precision of this distance ± 1 Å was determined from simulations of Q-band ED EPR spectrum with different ν_d values (see Figure S8). This distance is substantially smaller than $r = 20.4$ Å, which was obtained for the sodium sample.

It should be noted that the point–dipole values of the interspin distance measured in this work are “effective” distances between the centers of gravity of the spin densities on the flavosemiquinones. The spin density of flavin radicals is delocalized at the isoalloxazine ring³⁸ with its barycenter located at the central pyrazine ring, i.e., ≤ 3.6 Å from the edges of the isoalloxazine ring.³⁹ Thus, the FMN_{NqrB}–FMN_{NqrC} edge-to-edge distance should be changed from 16.8 ± 3.6 Å in the sodium sample to 11.7 ± 3.6 Å in the sodium-free sample, which should significantly enhance the electron transport rate between these prosthetic groups.

DISCUSSION

Although significant progress has been recently achieved in the studies of Na⁺-NQR, the mechanism of the sodium potential generation by the enzyme is still far from being understood. Conservation of the redox energy in the form of sodium transmembrane potential could take place if the reduction of a Na⁺-NQR cofactor is connected with the capture of Na⁺ from the cytoplasm as an electrostatic compensation effect, and the consequent oxidation of the cofactor in course of the catalytic cycle is coupled to the ejection of Na⁺ at the other side of membrane.^{5,21} If Na⁺-NQR uses just this mechanism of energy conservation, the redox potential of at least one of its cofactors should depend on the Na⁺ concentration. However, the midpoint potentials of all the redox transitions determined in Na⁺-NQR were found to be essentially independent from Na⁺ concentration.^{18,22,23} As an alternative mechanism of energy conservation by Na⁺-NQR, the following scheme of the enzyme functioning could be proposed (see Figure 7): (1) In the absence of bound Na⁺, FMN_{NqrC} is located close to FMN_{NqrB} and remote from the [2Fe–2S] cluster, so that the electron transfer between the [2Fe–2S] cluster and FMN_{NqrC} is too slow or even impossible (state *a*). (2) Na⁺ binding from the cytoplasmic side of the membrane results in a conformational change bringing the [2Fe–2S] cluster and FMN_{NqrC} close together, which allows the electron transfer between them. The same conformational change separates the two FMN residues, making impossible the electron transport between the flavins due to the long distance (state *b*). (3) Reduction of FMN_{NqrC} causes another conformational change switching the enzyme from the “inward facing” (cytoplasm-open) to the “outward facing” (periplasm-open) conformation (state *c*). (4) As sodium is released from the binding site at the periplasmic side of the membrane, FMN_{NqrC} moves back to take its position close to FMN_{NqrB}, allowing the electron transfer between the flavins (state *d*). (5) Oxidation of FMN_{NqrC} results in the reorientation of Na⁺-NQR back to its inward facing conformation, thus completing the cycle.

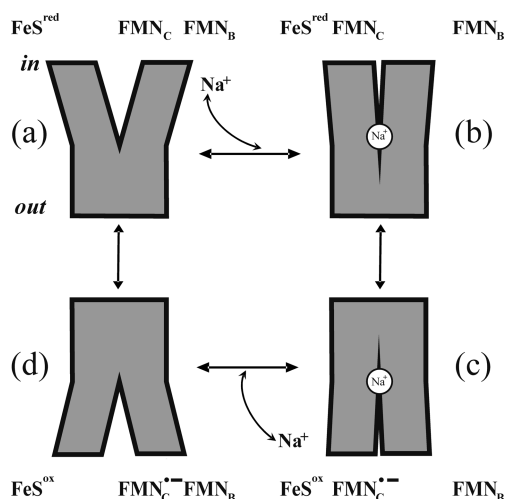


Figure 7. Proposed mechanism of the sodium potential generation by Na⁺-NQR. The details are discussed in the text. FMN_B and FMN_C depict FMN residues covalently bound to subunits NqrB and NqrC, respectively.

It is noteworthy that in this scheme the NqrC subunit with its bound FMN residue operates as a mobile shuttle transferring electrons and triggering conformational changes in the enzyme. In this scheme binding and release of Na⁺ are not driven by changes in Na⁺-NQR affinity to sodium ions but trapped *kinetically* by the electron transport. It does not imply any sodium dependence of redox potential of any prosthetic group but requires that the distances (and, as a result, the electron tunneling rates) between certain Na⁺-NQR prosthetic groups vary upon sodium binding.

In the present work, the interspin distance between two covalently bound FMN residues in Na⁺-NQR was determined in the absence and in the presence of sodium ions. We found this distance about 20.4 Å at high sodium concentration, while in the absence of Na⁺, FMN_{NqrC} and FMN_{NqrB} are brought together at 15.3 Å. Thus, the distance between two covalently bound FMN residues can vary by about 5 Å upon changes in Na⁺ concentration in the incubation medium, which is in line with the proposed scheme of Na⁺-NQR functioning (Figure 7).

It is noteworthy that not all the states of the proposed scheme are identified in the present work. For instance, the key state of the enzyme functioning when [2Fe–2S] cluster and FMN_{NqrC} are located in close proximity to each other (Figure 7b,c) was not observed in our experiments. The reason for that was that we could not detect any enhancement of electron spin relaxation of the FMNs radicals under any conditions studied (see above). It indicates that the real scheme of Na⁺-NQR functioning is more complex, and some its stages can arise during the catalytic cycle only as a result of consequent and ordered events; i.e., they are not accessible at conditions of thermodynamic equilibrium used in this study.

■ ASSOCIATED CONTENT

■ Supporting Information

Electron spin relaxation of anionic flavin radicals in Na⁺-NQR samples; EPR spectra of Na⁺-NQR samples with wide magnetic field scan; X-band Mims ENDOR spectra of Na⁺-NQR samples; two-pulse ESEEM spectra of anionic flavin radicals in Na⁺-NQR samples; description of the material included. This

material is available free of charge via the Internet at <http://pubs.acs.org>.

■ AUTHOR INFORMATION

Corresponding Author

*Tel +7(495) 9300086, Fax +7(495) 9390338, e-mail bogachev@genebee.msu.ru (A.V.B.); Tel +7(383) 3332297, Fax +7(383) 3307350, e-mail chemphy@kinetics.nsc.ru (L.V.K.).

Funding

This work was supported by the Russian Foundation for Basic Research (to A.V.B. and Y.V.B., project number 10-04-00352), the Academy of Finland, Biocentrum Helsinki, Magnus Ehrnrooth Foundation, and the Sigrid Jusélius Foundation (to D.A.B. and M.I.V.), and Ministry of Education and Science of Russian Federation (to L.V.K., project numbers 14.740.11.0369 and 11.519.11.1006).

Notes

The authors declare no competing financial interest.

[†]Deceased.

■ ACKNOWLEDGMENTS

This work is dedicated to the memory of our colleague and dear friend Michael Verkhovsky, who recently passed away. The authors thank Dr. Stefan Stoll for his helpful advice concerning the use of the EasySpin software and to Tatiana I. Pichugina for assistance in pulse EPR experiments and numerical calculations. We are also indebted to Prof. M. Wikström for helpful discussions and for critical reading of the manuscript.

■ ABBREVIATIONS

BTP, 1,3-bis[tris(hydroxymethyl)methylamino]propane; CW, continuous wave; DDM, *n*-dodecyl-β-D-maltoside; ED, echo-detected; *E*_h, ambient redox potential; ELDOR, electron–electron double resonance; *E*_m, midpoint redox potential; ENDOR, electron–nuclear double resonance; EPR, electron paramagnetic resonance; ESE, electron spin echo; ESEEM, electron spin echo envelope modulation; FT, Fourier transform; HEPES, *N*-(2-hydroxyethyl)piperazine-*N'*-(2-ethanesulfonic acid); HFI, hyperfine interactions; Na⁺-NQR, Na⁺-translocating NADH:quinone oxidoreductase; rf, radio frequency; SHE, standard hydrogen electrode.

■ REFERENCES

- (1) Verkhovsky, M. I., and Bogachev, A. V. (2010) Sodium-translocating NADH:quinone oxidoreductase as a redox-driven ion pump. *Biochim. Biophys. Acta* 1797, 738–746.
- (2) Zhou, W., Bertsova, Y. V., Feng, B., Tsatsos, P., Verkhovskaya, M. L., Gennis, R. B., Bogachev, A. V., and Barquera, B. (1999) Sequencing and preliminary characterization of the Na⁺-translocating NADH:ubiquinone oxidoreductase from *Vibrio harveyi*. *Biochemistry* 38, 16246–16252.
- (3) Hase, C. C., Fedorova, N. D., Galperin, M. Y., and Dibrov, P. A. (2001) Sodium ion cycle in bacterial pathogens: evidence from cross-genome comparisons. *Microbiol. Mol. Biol. Rev.* 65, 353–370.
- (4) Nakayama, Y., Hayashi, M., and Unemoto, T. (1998) Identification of six subunits constituting Na⁺-translocating NADH:quinone reductase from the marine *Vibrio alginolyticus*. *FEBS Lett.* 422, 240–242.
- (5) Rich, P. R., Meunier, B., and Ward, F. B. (1995) Predicted structure and possible ionmotive mechanism of the sodium-linked NADH-ubiquinone oxidoreductase of *Vibrio alginolyticus*. *FEBS Lett.* 375, 5–10.

- (6) Hayashi, M., Hirai, K., and Unemoto, T. (1995) Sequencing and the alignment of structural genes in the *nqr* operon encoding the Na⁺-translocating NADH:quinone reductase from *Vibrio alginolyticus*. *FEBS Lett.* 363, 75–77.
- (7) Turk, K., Puhar, A., Neese, F., Bill, E., Fritz, G., and Steuber, J. (2004) NADH oxidation by the Na⁺-translocating NADH:quinone oxidoreductase from *Vibrio cholerae*: functional role of the NqrF subunit. *J. Biol. Chem.* 279, 21349–21355.
- (8) Barquera, B., Nilges, M. J., Morgan, J. E., Ramirez-Silva, L., Zhou, W., and Gennis, R. B. (2004) Mutagenesis study of the 2Fe-2S center and the FAD binding site of the Na⁺-translocating NADH:ubiquinone oxidoreductase from *Vibrio cholerae*. *Biochemistry* 43, 12322–12330.
- (9) Nakayama, Y., Yasui, M., Sugahara, K., Hayashi, M., and Unemoto, T. (2000) Covalently bound flavin in the NqrB and NqrC subunits of Na⁺-translocating NADH:quinone reductase from *Vibrio alginolyticus*. *FEBS Lett.* 474, 165–168.
- (10) Hayashi, M., Nakayama, Y., Yasui, M., Maeda, M., Furuishi, K., and Unemoto, T. (2001) FMN is covalently attached to a threonine residue in the NqrB and NqrC subunits of Na⁺-translocating NADH:quinone reductase from *Vibrio alginolyticus*. *FEBS Lett.* 488, 5–8.
- (11) Barquera, B., Zhou, W., Morgan, J. E., and Gennis, R. B. (2002) Riboflavin is a component of the Na⁺-pumping NADH:quinone oxidoreductase from *Vibrio cholerae*. *Proc. Natl. Acad. Sci. U. S. A.* 99, 10322–10324.
- (12) Juárez, O., Nilges, M. J., Gillespie, P., Cotton, J., and Barquera, B. (2008) Riboflavin is an active redox cofactor in the Na⁺-pumping NADH:quinone oxidoreductase (Na⁺-NQR) from *Vibrio cholerae*. *J. Biol. Chem.* 283, 33162–33167.
- (13) Casutt, M. S., Huber, T., Brunisholz, R., Tao, M., Fritz, G., and Steuber, J. (2010) Localization and function of the membrane-bound riboflavin in the Na⁺-translocating NADH:quinone oxidoreductase (Na⁺-NQR) from *Vibrio cholerae*. *J. Biol. Chem.* 285, 27088–27099.
- (14) Bogachev, A. V., Bertsova, Y. V., Barquera, B., and Verkhovsky, M. I. (2001) Sodium-dependent steps in the redox reactions of the Na⁺-motive NADH:quinone oxidoreductase from *Vibrio harveyi*. *Biochemistry* 40, 7318–7323.
- (15) Bogachev, A. V., Bertsova, Y. V., Ruuge, E. K., Wikström, M., and Verkhovsky, M. I. (2002) Kinetics of the spectral changes during reduction of the Na⁺-motive NADH:quinone oxidoreductase from *Vibrio harveyi*. *Biochim. Biophys. Acta* 1556, 113–120.
- (16) Barquera, B., Hellwig, P., Zhou, W., Morgan, J. E., Hase, C. C., Gosink, K. K., Nilges, M., Bruesehoff, P. J., Roth, A., Lancaster, C. R., and Gennis, R. B. (2002) Purification and characterization of the recombinant Na⁺-translocating NADH:quinone oxidoreductase from *Vibrio cholerae*. *Biochemistry* 41, 3781–3789.
- (17) Barquera, B., Ramirez-Silva, L., Morgan, J. E., and Nilges, M. J. (2006) A new flavin radical signal in the Na⁺-pumping NADH:quinone oxidoreductase from *Vibrio cholerae*. *J. Biol. Chem.* 281, 36482–36491.
- (18) Bogachev, A. V., Kulik, L. V., Bloch, D. A., Bertsova, Y. V., Fadeeva, M. S., and Verkhovsky, M. I. (2009) Redox properties of the prosthetic groups of Na⁺-translocating NADH:quinone oxidoreductase. 1. EPR study of the enzyme. *Biochemistry* 48, 6291–6298.
- (19) Bogachev, A. V., Belevich, N. P., Bertsova, Y. V., and Verkhovsky, M. I. (2009) Primary steps of Na⁺-translocating NADH:ubiquinone oxidoreductase catalytic cycle resolved by the ultra-fast freeze-quench approach. *J. Biol. Chem.* 284, 5533–5538.
- (20) Juárez, O., Morgan, J. E., and Barquera, B. (2009) The electron transfer pathway of the Na⁺-pumping NADH:quinone oxidoreductase from *Vibrio cholerae*. *J. Biol. Chem.* 284, 8963–8972.
- (21) Bogachev, A. V., and Verkhovsky, M. I. (2005) Na⁺-Translocating NADH:quinone oxidoreductase: progress achieved and prospects of investigations. *Biochemistry (Moscow)* 70, 143–149.
- (22) Bogachev, A. V., Bertsova, Y. V., Bloch, D. A., and Verkhovsky, M. I. (2006) Thermodynamic properties of the redox centers of Na⁺-translocating NADH:quinone oxidoreductase. *Biochemistry* 45, 3421–3428.
- (23) Bogachev, A. V., Bloch, D. A., Bertsova, Y. V., and Verkhovsky, M. I. (2009) Redox properties of the prosthetic groups of Na⁺-translocating NADH:quinone oxidoreductase. 2. Study of the enzyme by optical spectroscopy. *Biochemistry* 48, 6299–6304.
- (24) Harder, S. R., Feinberg, B. A., and Ragsdale, S. W. (1989) A spectroelectrochemical cell designed for low temperature electron paramagnetic resonance titration of oxygen-sensitive proteins. *Anal. Biochem.* 181, 283–287.
- (25) Pannier, M., Veit, S., Godt, A., Jeschke, G., and Spiess, H. W. (2000) Dead-time free measurement of dipole-dipole interactions between electron spins. *J. Magn. Reson.* 142, 331–340.
- (26) Kulik, L. V., Pivtsov, A. A., and Bogachev, A. V. (2010) Pulse EPR, ENDOR, and ELDOR study of anionic flavin radicals in Na⁺-translocating NADH:quinone oxidoreductase. *Appl. Magn. Reson.* 37, 353–361.
- (27) Gulla, A. F., and Budil, D. E. (2001) Orientation dependence of electric field effects in the g-factor of nitroxides measured by 220 GHz EPR. *J. Phys. Chem. B* 105, 8056–8063.
- (28) Schweiger, A., and Jeschke, G. (2001) *Principles of Pulse Electron Paramagnetic Resonance*, Oxford University Press, Oxford.
- (29) Dikanov, S. A., and Tsvetkov, Yu. D. (1992) *Electron Spin Echo Modulation (ESEEM) Spectroscopy*, CRC Press, Boca Raton, FL.
- (30) Milov, A. D., Salikhov, K. M., and Shirov, M. D. (1981) Application of ELDOR in electron-spin echo for paramagnetic center space distribution in solids. *Fiz. Tverd. Tela* 23, 975–982.
- (31) Milov, A. D., Ponomarev, A. B., and Tsvetkov, Yu. D. (1984) Electron-electron double resonance in electron spin echo: Model biradical systems and the sensitized photolysis of decalin. *Chem. Phys. Lett.* 110, 67–72.
- (32) Kay, C. W. M., Elsässer, C., Bittl, R., Farrell, S. R., and Thorpe, C. (2006) Determination of the distance between the two neutral flavin radicals in augments of liver regeneration by pulsed ELDO. *J. Am. Chem. Soc.* 128, 76–77.
- (33) Swanson, M. A., Kathirvelu, V., Majtan, T., Frerman, F. E., Eaton, G. R., and Eaton, S. S. (2009) DEER distance measurement between a spin label and a native FAD semiquinone in electron transfer flavoprotein. *J. Am. Chem. Soc.* 131, 15978–15979.
- (34) Milov, A. D., Maryasov, A. G., and Tsvetkov, Yu. D. (1998) Pulsed electron double resonance (PELDOR) and its applications in free-radicals research. *Appl. Magn. Reson.* 15, 107–143.
- (35) Milov, A. D., Maryasov, A. G., and Tsvetkov, Yu. D. (2004) The effect of microwave pulse duration on the distance distribution function between the spin labels obtained by PELDOR data analysis. *Appl. Magn. Reson.* 26, 587–599.
- (36) Barquera, B., Morgan, J. E., Lukoyanov, D., Scholes, C. P., Gennis, R. B., and Nilges, M. J. (2003) X- and W-band EPR and Q-band ENDOR studies of the flavin radical in the Na⁺-translocating NADH:quinone oxidoreductase from *Vibrio cholerae*. *J. Am. Chem. Soc.* 125, 265–275.
- (37) Stoll, S., and Schweiger, A. (2006) EasySpin, a comprehensive software package for spectral simulation and analysis in EPR. *J. Magn. Reson.* 178, 42–55.
- (38) Garcia, J. I., Medina, M., Sancho, J., Alonso, P. J., Gomez-Moreno, C., Mayoral, J. A., and Martinez, J. I. (2002) Theoretical analysis of the electron spin density distribution of the flavin semiquinone isalloxazine ring within model protein environments. *J. Phys. Chem. A* 106, 4729–4735.
- (39) Fielding, A. J., Usselman, R. J., Watmough, N., Simkovic, M., Frerman, F. E., Eaton, G. R., and Eaton, S. S. (2008) Electron spin relaxation enhancement measurements of interspin distances in human, porcine, and *Rhodobacter* electron transfer flavoprotein-ubiquinone oxidoreductase (ETF-QO). *J. Magn. Reson.* 190, 222–232.